Available online at www.sciencedirect.com
ScienceDirect
Polymer 47 (2006) 8147–8154
polymer
www.elsevier.com/locate/polymer

On the structure of holographic polymer-dispersed polyethylene glycol

Michael J. Birnkrant [a], Hilary K. McWilliams [a], Christopher Y. Li [a,*], Lalgudi V. Natarajan [b], Vincent P. Tondiglia [b], Richard L. Sutherland [b], Pamela F. Lloyd [c], Timothy J. Bunning [d,**]

[a] *A. J. Drexel Nanotechnology Institute and Department of Materials Science and Engineering, Drexel University, LeBow Building, Room 443, 3141 Chestnut Street, Philadelphia, PA 19104, USA*
[b] *Science Applications International Corporation, 4031 Colonel Glenn Highway, Dayton, OH 45431, USA*
[c] *UES, Inc., 4401 Dayton-Xenia Road, Dayton, OH 45432, USA*
[d] *Air Force Research Laboratory, Materials and Manufacturing Directorate, Wright-Patterson Air Force Base, OH 45433, USA*

Received 23 August 2006; received in revised form 17 September 2006; accepted 18 September 2006
Available online 16 October 2006

Abstract

Holographic polymerization (H-P) has been used to fabricate polymer-dispersed liquid crystals and pattern inert nanoparticles. In this article, one-dimensional grating structures of Norland resin and polyethylene glycol (PEG) were achieved using the H-P technique. Both reflection and transmission grating structures were fabricated. The optical properties of the reflection grating structures (also known as Bragg reflectors, BRs) are thermosensitive, which is attributed to the formation and crystallization of PEG crystals. The thermal switching temperature of the BR can be tuned by using different molecular weight PEG samples. The hierarchical structure and morphology of the BR were studied using synchrotron X-ray, polarized light microscopy and transmission electron microscopy. PEG crystals were found to be confined in ~60 nm thick layers in the BR. Upon crystallization, the PEG lamellae were parallel to the BR surfaces and PEG chains were parallel to the BR normal, resembling the confined crystallization behavior of polyethylene oxide (PEO) in PEO-*block*-polystyrene (PEO-*b*-PS) block copolymers. This observation suggests that the tethering effect in the block copolymer systems does not play a major role in PEG chain orientation in the confined nanoenvironment.

Keywords: Holographic polymerization; Nanoconfinement; Polymer crystallization

1. Introduction

A number of different methods, including colloid crystal assembly, lithography techniques and block copolymer (BCP) self-assembly, have been used to fabricate wavelength scale photonic structures in order to mold the flow of light [1–6]. A drawback of these techniques is the required lengthy sample preparation. In the latter case, defects inherent in BCPs hinder the formation of large-scale structures although a number of methods have been proposed [7–10]. Recently, holographic photopolymerization (H-P) has been proven to be a simple, fast and attractive means to fabricate one-, two- and three-dimensional (1D, 2D, 3D) complex photonic structures at a relatively large-scale [6,11–14]. During the H-P process, a photopolymerizable syrup is exposed to two or more coherent, interfering laser beams, which create a standing wave pattern. Higher intensity regions within the standing wave result in a locally faster polymerization process, which leads to a spatial distribution of high molecular weight (MW) polymers. Pure polymer films with a periodic refractive index (RI) modulation normal to the film surface (reflection geometry) were first fabricated several decades ago [15–17]. This unique technique was extended in the mid-90s by including low molar mass, anisotropic liquid crystals (LCs) in the polymerization syrup. Non-reactive LCs, normally ~20–30 (w/w)% of the syrup, are mixed with photopolymerizable monomers, initiators and surfactants. H-P of this mixture leads to periodically patterned, nanoscale LC droplets, a structure known as holographic polymer-dispersed liquid crystals (HPDLC) [11]. The RI contrast

* Corresponding author. Tel.: +1 215 895 2083; fax: +1 215 895 6760.
** Corresponding author.
E-mail addresses: chrisli@drexel.edu (C.Y. Li), timothy.bunning@wpafb.af.mil (T.J. Bunning).

0032-3861/$ - see front matter © 2006 Elsevier Ltd. All rights reserved.
doi:10.1016/j.polymer.2006.09.052

can be easily controlled by applying external electric fields and the optical properties of HPDLC can thus be modulated. Novel 3D photonic crystal structures were also formed by using a multiple-beam set-up [12,13,18–20].

Due to the fast kinetics of photopolymerization, these holographic structures can be fabricated within seconds and the symmetry, dimensionality, size and RI modulation can be easily controlled by the fabrication conditions. In addition to patterning LCs, a variety of nanosized objects have also been patterned into ordered photonic structures [21]. In theory, if the nanosize objects do not affect the polymerization process, they could be patterned into ordered structures using the H-P method. However, phase separation during the photopolymerization process is rather complicated and often times, the rate of phase separation between the crosslinked resins/monomers and the to-be-patterned objects has to occur at a similar rate as photopolymeriztion. Miscibility and viscosity dictate the phase separation kinetics, which, in turn, account for the formation of the ordered nanostructures. By replacing the LC with gold nanoparticles (5 nm in diameter), polystyrene (PS), latex spheres (260 nm diameter) or silicate nanoplates, H-P led to 1D structures with spatially patterned nanoparticles and the periodicity is approximately a few hundreds of nanometers [21].

We recently investigated reflection grating structures—BR—formed by H-P of a syrup containing photopolymerizable monomers (Norland resin), initiators and an inert polymer, polyethylene glycol (PEG) [22]. Using PEG to replace previously reported LC/nanoparticles, uniform 1D BR structures could also be formed, although PEG molecules are much larger in size than that of small molecular mass LCs. The grating was formed due to the lamellar ordering of crosslinked Norland resin and semi-continuous layers of PEG. Interestingly, the reflecting wavelength red shifts approximately 20 nm while the diffraction efficiency (DE) concurrently increases upon heating. This thermoswitching behavior was attributed to the PEG crystal formation and melting during the cooling and heating processes. The structure and crystallization behavior of PEG BR are investigated in this paper. PEG/Norland BR with different MW PEG thermally switched and transmission optical structures of PEG/Norland were fabricated. The transition temperature depends on the PEG MW. Detailed synchrotron X-ray studies show that the holographic polymer-dispersed polymer (HPDP) structure provides nanoconfinement during the PEG crystal structure formation. All the PEG crystals confined by HPDP investigated contained PEG chains that are exclusively parallel to the BR normal. Comparisons of the HPDP structure with the previously investigated nanoconfined crystallization of PEO in block copolymers are discussed.

2. Experimental

2.1. Materials

The formulation of the prepolymer syrup consisted of 15–30 (w/w)% PEG, 65–80% crosslinkable monomer and 3–5% photoinitiators. PEG with MW 2000, 4600, 8000 g/mol was purchased from Aldrich Co. The crosslinkable polymer was a commercially available thiol-ene polymer known as Norland Optical Adhesive 65 and Norland Blocking Adhesive 107 from Norland Products Inc. The photoinitiator was Darocure© 4265 from CIBA-GEIGY company. All the materials were used as received.

2.2. Formation of holographic Bragg grating

The fabrication of reflection gratings was achieved using a Coherent Ar-ion laser (model Sabre Innova 10R/2) with a laser wavelength of 363.8 nm and an output power of ~300 mW using a single beam configuration as shown in Fig. 1a. The interference pattern that arises from the internal reflection of the beam on the hypotenuse of an isosceles 90° glass prism results in the formation of a grating. The cell was placed in optical contact with the prism hypotenuse using an index-matching fluid and the exposure time was typically 30–60 s. The prism and the cell assembly were placed on a rotation stage to change the notch wavelength. Transmission gratings can also be obtained in the present system; the laser set-up for the transmission grating writing is shown in Fig. 1b. A diffuse UV laser was split into two beams using the prism and these beams were converged on the BR cell forming a grating.

2.3. Characterization

Bright-field transmission electron microscopy (BFTEM) was performed on a JEOL 2000FX TEM with an accelerating voltage of 120 kV. A Reichert Ultracut cryo-ultramicrotome was used to microtome the BR sample with a DiATOME 35° diamond knife. Thin sections of 60 nm of the sample were cut and floated on the water surface and subsequently collected on a TEM copper grid.

Polarized light microscopy (PLM) was performed on an Olympus BX-51 coupled with a Mettler–Toledo hot stage FP-90. The image was captured using an Insight digital camera. Isothermal characterization was carried out by preheating

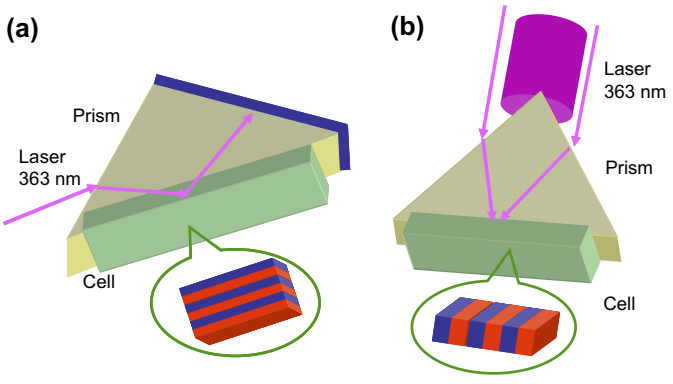

Fig. 1. Experimental set-up for one prism: (a) reflection grating and (b) transmission grating writing.

gratings on a hotplate at 90 °C and then transferred to a Mettler–Toledo hot stage for observation.

Optical characterization of the reflection gratings was carried out using an Ocean Optics fiber spectrometer. A white light source coupled to a fiber-optic delivery system was used as the light source.

2D SAXS experiments were carried out at the synchrotron X-ray beamline X27C at the National Synchrotron Light Source in Brookhaven National Laboratory. The zero pixel of the 2D SAXS pattern was calibrated using silver behenate with the first-order scattering vector q being 1.076 nm^{-1}. The air scattering was subtracted. The X-ray beam spot was 0.1 mm in diameter. The X-ray beam was aligned parallel to the *surface* and *normal* directions of the sample. 2D WAXD patterns were also recorded at room temperature in the same set-up with the sample to detector distance of ~15 cm.

3. Results and discussion

3.1. Temperature sensitive Bragg grating from PEG/Norland

A 1D BR was written using a single beam configuration as previously discussed. Fig. 2a shows the transmission spectra of PEG/Norland grating with different MWs. Reflection peaks with modest diffraction efficiency (~30%) can be seen. The notch position is ~600–610 nm, which can be tuned by changing the incident angles of the set-up. The formation of DE indicates a RI modulation in the BR, which is due to the spatial distribution of crosslinked photopolymer and PEG. Thin cross sections (~60 nm thick) were obtained by ultramicrotoming along the film normal direction at room temperature. Fig. 2b shows a TEM micrograph of a thin section of the grating of Norland 65 and PEG 2000. Similar to previously reported PEG 4600/Norland 65 sample, a long range uniform layered structure, with alternating dark and light regions is evident from the micrograph. Unlike holographic polymer-dispersed liquid crystal systems, which form droplets of 100–200 nm in diameter confined within the polymer matrix, the PEG layers form a continuous layered structure with a lamellar spacing of ~200 nm. The unique morphology may be due to a slower phase separation process of PEG and Norland during polymerization as opposed to LC/Norland systems.

In the previous study, the notch position as well as the DE of these HPDP films could be modulated by varying the temperature: as the temperature increases, both the notch position and the DE increase and the reverse occurs upon cooling [22]. This is due to PEG going through a crystal–melt transition, the volume increases and the BR grating expands, which in turn, leads to a red shift of the notch as observed in the transmission spectra. Furthermore, the RI of PEG is smaller in the amorphous state. Since the RI of the Norland resin is higher than that of PEG, decreasing PEG RI leads to an increase of the RI contrast between the Norland resin and the PEG layer; this dramatically increased the DE of the BR. The melting points of the PEG crystal depend on the polymer molecular structure such as MW leading to the speculation that different MW PEG BRs might have different thermoswitching temperatures.

In order to confirm this hypothesis, three different MW PEG samples were used for the thermal switching experiments. Fig. 3 shows the notch/DE vs. temperature plots for PEG 2000/Norland, PEG 4600/Norland, and PEG 8000/Norland systems. Fig. 3a, c and e exhibits the characteristic red shift and increase in DE during the heating cycle while

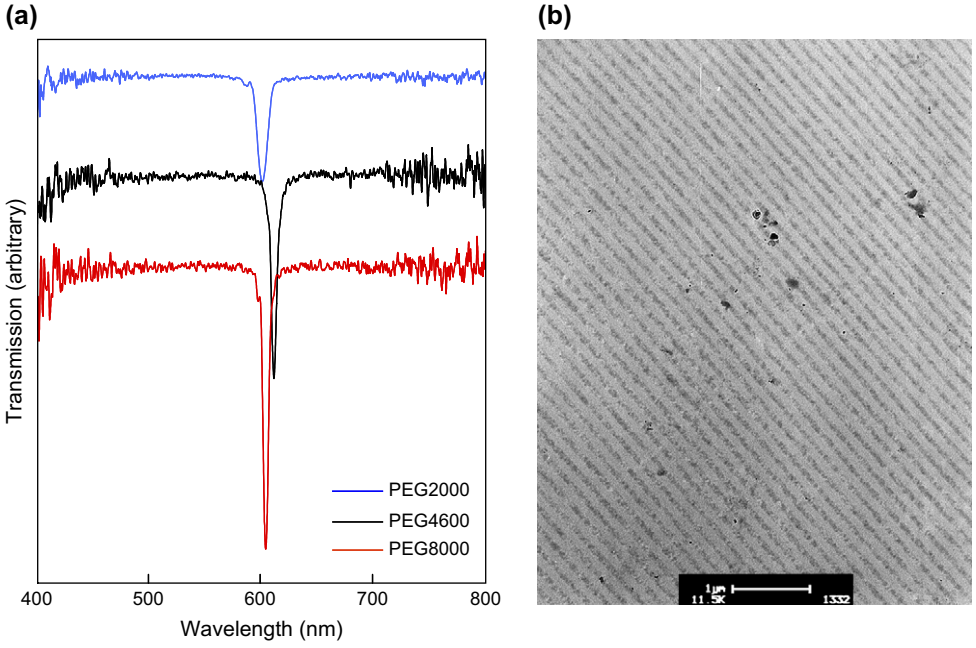

Fig. 2. (a) Transmission spectra of the reflection gratings of PEG and Norland 65 adhesives. The baselines have been offset for clarity in display of the spectra. (b) TEM micrograph of a thin section of a PEG 2000/Norland 65 reflection grating.

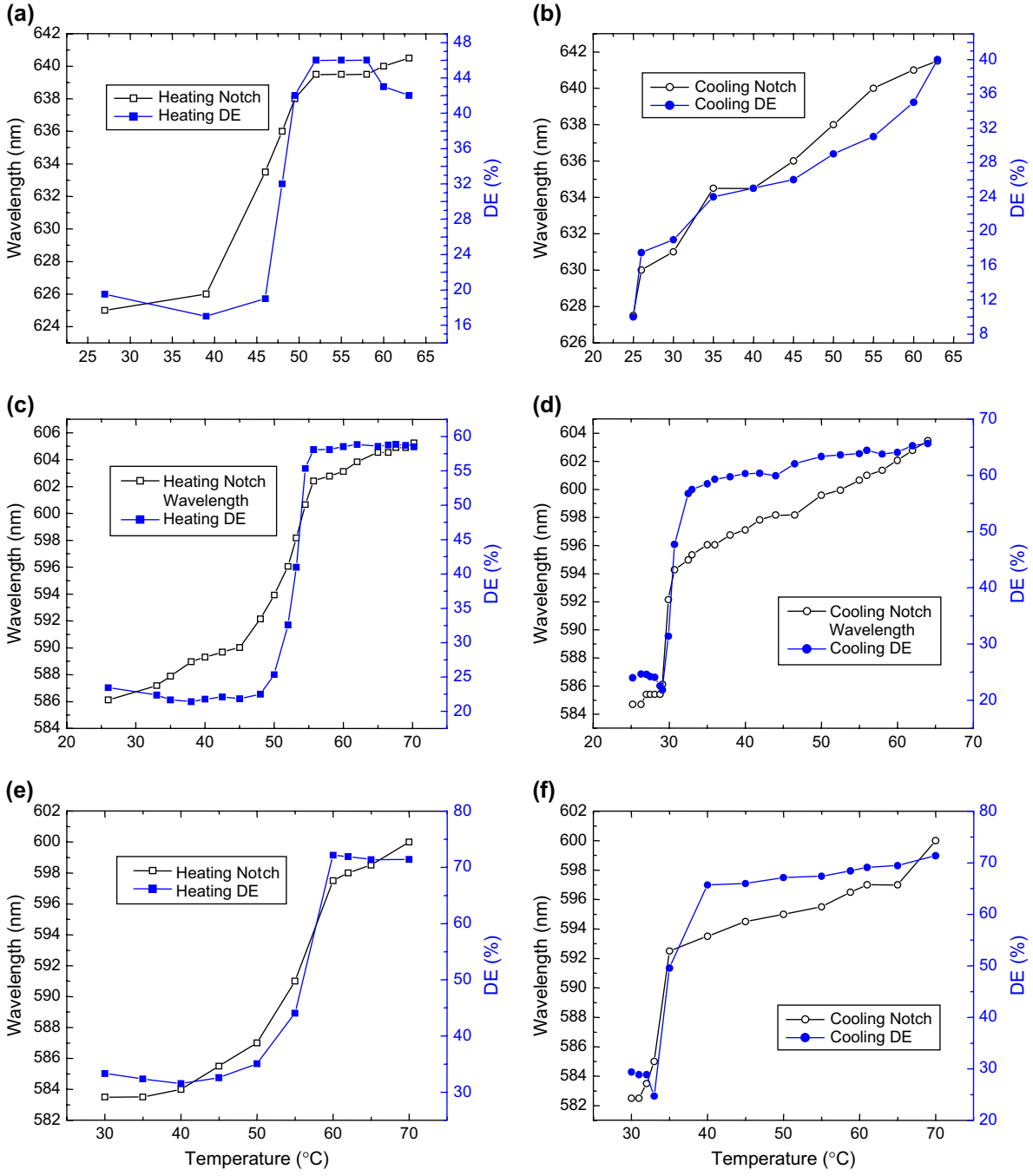

Fig. 3. Plots of the notch position and DE change with respect to temperature in transmission spectra of the PEG/Norland 65 systems: (a) PEG 2000/Norland 65 on heating; (b) PEG 2000/Norland 65 on cooling; (c) PEG 4600/Norland 65 on heating; (d) PEG 4600/Norland 65 on cooling; (e) PEG 8000/Norland 65 on heating; (f) PEG 8000/Norland 65 on cooling.

Fig. 3b, d and f show the reverse effects of the cooling process. The transition temperatures can be identified as 46 °C, 50 °C and 57 °C upon heating PEG 2000/Norland, PEG 4600/Norland, and PEG 8000/Norland samples. Upon cooling, PEG 4600/Norland and PEG 8000/Norland showed 30 °C and 35 °C transitions. The various switching temperatures can be attributed to the different melting points of the PEG/Norland gratings. The PEG 2000/Norland BR cooling curve shows that the notch position and DE do not have a sharp change, but a gradual decrease in DE and notch position. This is attributed to the slow crystallization kinetics of the PEG 2000 in the HPDP at room temperature. Therefore, a thermosensitive BR with the switching temperatures ranging from 30 °C to 57 °C can be readily obtained.

Transmission grating based on PEG and Norland resin was also achieved using the set-up previously discussed and the DE was measured to be ~1.5%. The Bragg diffraction angle was ~46°, leading to a *d*-spacing of 439 nm, which was confirmed

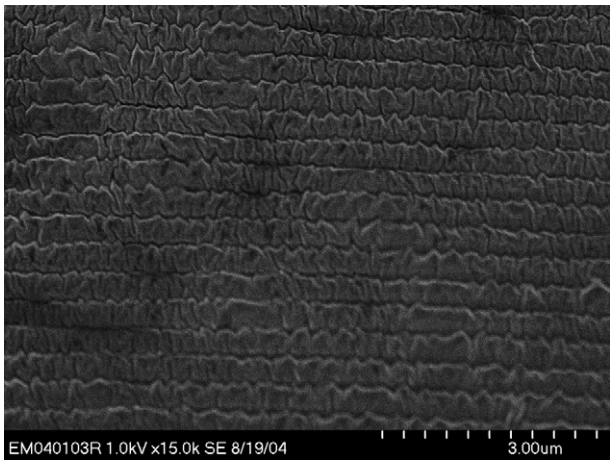

Fig. 4. SEM micrograph of the surface of a PEG/Norland transmission grating.

by the SEM results. Fig. 4 shows a SEM micrograph of the surface of transmission grating of PEG 400 (19%)/methanol (10%)/Norland 107 (68%)/Darocure© 4265 (3%). Methanol was added to decrease the system viscosity. A 1D layer structure can be seen from the figure, indicating that PEG was patterned using the H-P technique with the transmission grating geometry (note that this sample was not microtomed). The transmission grating shows the buckling effect along the layer direction, this may be attributed to the shrinkage of the grating structure after methanol evaporated. A detailed study is ongoing to quantitatively understand the relationship between the buckling and the methanol contents.

3.2. PEG phase structure and morphology in the confined HPDP

Since PEG molecules are confined within the crosslinked Norland resin layers, the present BR also provides an excellent system to study the confined crystallization behavior of PEG. Synchrotron X-ray diffraction and PLM experiments were employed. The HPDP cell was opened using a razor knife and thin, free-standing films (~10 μm) were obtained. This film was subjected to 2D XRD studies. Fig. 5 shows the XRD pattern of PEG/Norland BRs with X-ray aligning parallel (Fig. 5a, c, e and g), and perpendicular (Fig. 5b, d, f and h) to the gratings, respectively. Fig. 5a and b is schematic representation of the experimental set-up. In Fig. 5c, e and g the XRD patterns show orientation while in Fig. 5d, f and h only ring patterns were obtained. Detailed investigation determined that the inner diffraction arcs can be assigned as (120) with a *d*-spacing of 0.494 nm and the outer diffraction can be assigned as the overlap of (−132), (032), (112), (−212), (124), (−204), and (004) reflections with a *d*-spacing of 0.398 nm. From Fig. 5c, e and g it is clear that the (120) diffractions are located on the meridian direction while the outer (−132), (032), (112), (−212), (124), (−204), and (004) reflections are located in the quadrants, as shown in the azimuthal scan (Fig. 6). Note that in the parallel alignment, the BR film is parallel to the X-ray and the meridian direction; all the (120) planes are parallel to the equator of the XRD pattern. While the unorientated diffraction patterns in the perpendicular set-up indicate that the PEG crystals do not have any in-plane orientation. Combining these two diffraction patterns, one can conclude that in the patterned regions of the HPDP, PEG forms lamellar crystals and all the PEG chains are perpendicular to the HPDP BR surface.

Fig. 7 shows the PLM observation of the PEG HPDP structures. All the polymers were dissolved in the monomer syrup before writing (for PEG 8000, heating was applied to ensure the homogeneous syrup); solidification/crystallization occurs during/after polymerization. It was observed that for the as-written samples, both the grating region and the unpatterned region show grainy texture while the grating areas have much lower birefringence. After melt and recrystallization, 2D spherulitical growth was observed in both sections, and the unpatterned region retains a higher birefringence than the patterned area. Multilayer growth can be observed in the grating as shown in Fig. 7. This may be due to the crystal growing in different layers of the grating. The relatively weak birefringence in the patterned region suggests that polymer chains are parallel to the film normal resulting in weak in-plane birefringence. The PLM observation is thus consistent with the XRD results.

Fig. 8 shows the schematic representation of the hierarchical structures of the PEG/Norland BR. On the ~60 nm level, lamellar layered structures with two crosslinked Norland layers confining PEG molecules between them provide hard nanoconfinement. Upon crystallization, PEG chains are parallel to the layer normal and the (120) planes are perpendicular to the layer surface. Confinement growth of polymer single crystal has been extensively studied in block copolymer systems. Crystal orientation was observed to depend upon the crystallization conditions and the same crystal orientation was observed for recrystallizing PEO-*b*-PS sample (M_n^{PEO} ~ 8.7K and M_n^{PS} ~ 9.2K) at temperatures higher than 35 °C [23]. The lamellar periodicity is ~18.7 nm. In the present case, the HPDP structure possesses a much larger scale compared to the previous block copolymer systems, indicating that the nanoconfinement effect can also be observed at ~60 nm scale. Furthermore, the PEG molecules are not tethered to the Norland matrix. The previous argument regarding the tethered junction of BCPs could induce a near perpendicular orientation to the inter-material dividing surface can be excluded in the present case. The perpendicular chain orientation of the PEG crystal appears to be in a thermodynamically more stable state. The in-plane orientation of the PEG allows the ⟨120⟩ direction of the PEG to be parallel with the HPDP surface, leading to much larger, more stable polymer crystals. In contrast, tilted or parallel chain orientation would lead to a ⟨120⟩ direction that is oblique/perpendicular to the HPDP surface, the crystal would quickly meet the solid confinement wall of the HPDP. Large size crystals are thus prohibited, which in turn, reduce the overall stability of the crystals. Thus, nanoconfinement effect on PEG crystallization was confirmed in the current HPDP system.

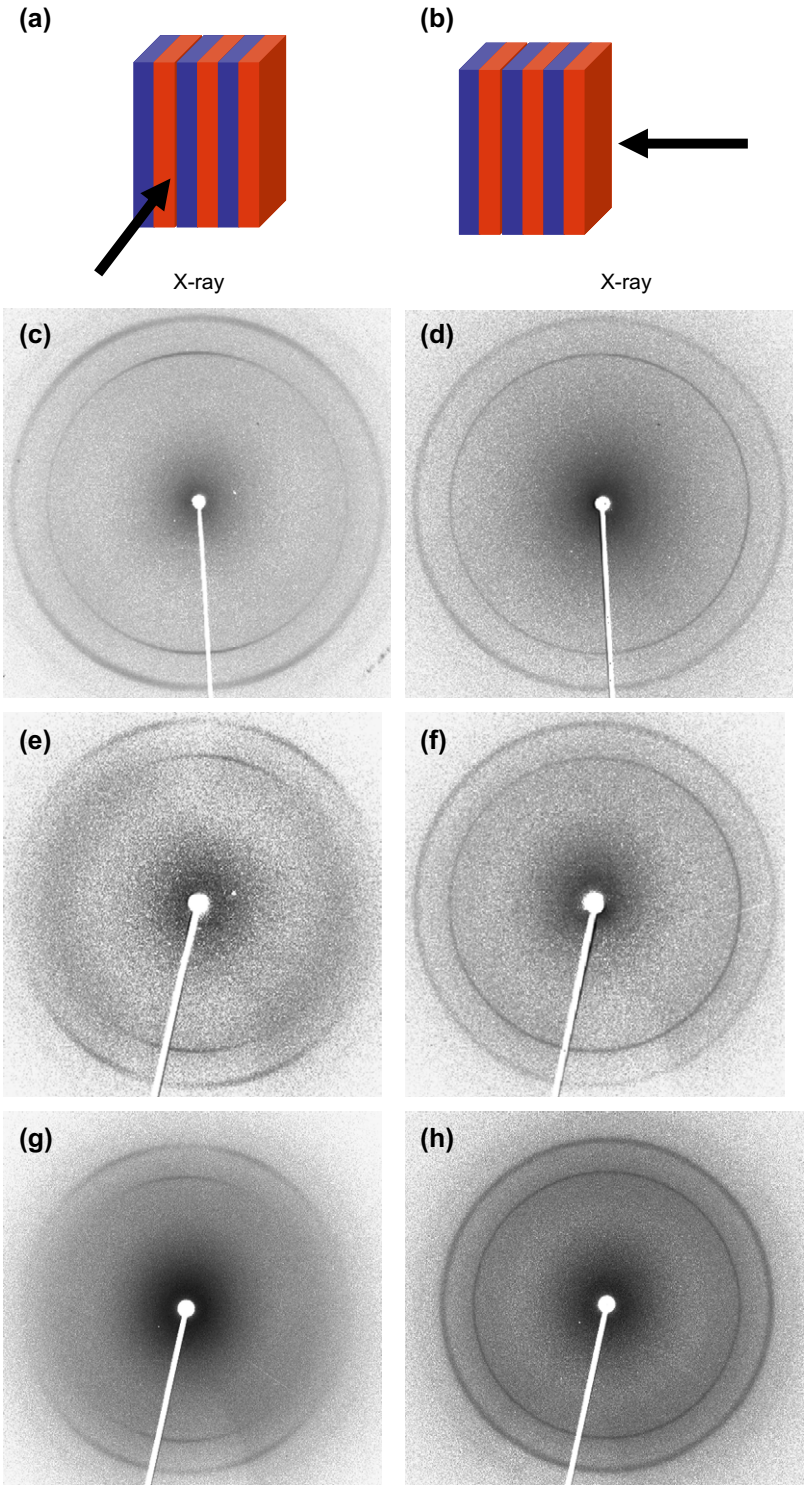

Fig. 5. 2D X-ray pattern of PEG/Norland grating: (a) X-ray set-up for parallel setting; (b) X-ray set-up for perpendicular setting; (c) 2D X-ray pattern for parallel setting PEG 2000/Norland; (d) 2D X-ray pattern for perpendicular setting PEG 2000/Norland; (e) 2D X-ray pattern for parallel setting PEG 4600/Norland; (f) 2D X-ray pattern for perpendicular setting PEG 4600/Norland; (g) 2D X-ray pattern for parallel setting PEG 8000/Norland; (h) 2D X-ray pattern for perpendicular setting PEG 8000/Norland.

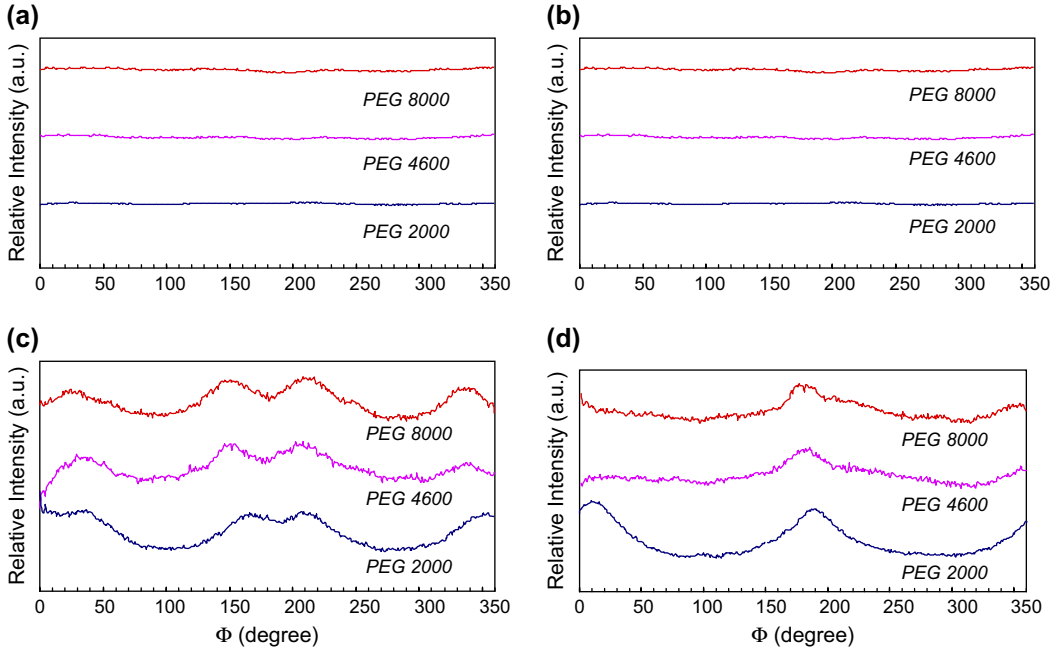

Fig. 6. Azimuthal scans of the 2D XRD patterns in Fig. 5: (a) perpendicular setting of PEG/Norland BR, outer ring d-spacing = 0.398 nm; (b) perpendicular setting of PEG/Norland BR, inner ring d-spacing = 0.494 nm; (c) parallel setting of PEG/Norland BR, outer ring d-spacing = 0.398 nm; (d) parallel setting of PEG/Norland BR, inner ring d-spacing = 0.494 nm.

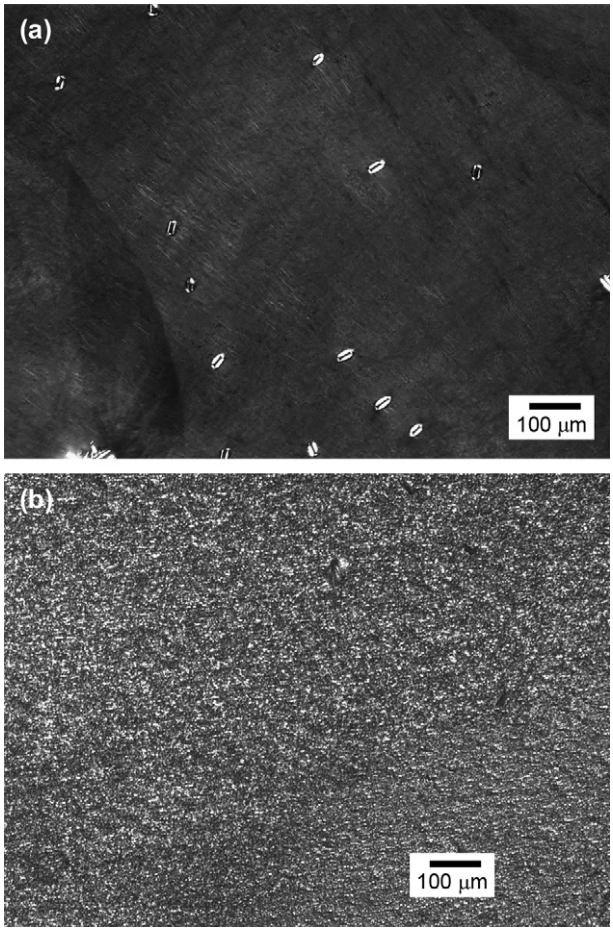

Fig. 7. PLM micrograph of PEG 4600/Norland/BR: (a) grating area and (b) non-grating area.

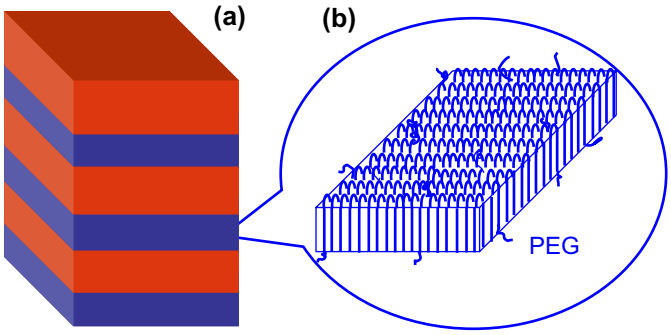

Fig. 8. Schematic representation of the hierarchical structure of PEG/Norland BR: (a) lamellar structures are formed with a periodicity of ~200 nm; (b) within the PEG layers, PEG crystals are formed and the lamellar crystals are parallel to the BR surface and the PEG chains are parallel to the BR normal.

4. Conclusion

BR structures were fabricated using H-P of several PEG/Norland systems. Uniform lamellar structures were formed with periodicity ~200 nm. The RI modulation between Norland resin and PEG led to the observation of a reflection notch in the transmission spectra. The notch position and the DE can be thermally shifted. The switching temperature was determined by the melting and crystallization temperatures of PEG. In addition, the switching temperature was also tuned by using different MW PEGs; switching temperatures from 30 °C to 57 °C were obtained. Both reflection and transmission grating structures were achieved. The hierarchical structure of the BR and PEG crystal was studied using synchrotron X-ray and the PEG crystal lamellae were parallel to

the BR surface and the chain axis was parallel to the BR normal. Compared to the confined crystallization of PEO studied in the block copolymer cases, the current system possesses larger nanodomain thickness and the PEG chains are not tethered to the interface. The orthogonal orientation of the lamellae is attributed to the thermodynamic stable state of the HPDP system.

Acknowledgements

MJB would like to thank NSF GK-12 award 0538476, NSF-IGERT Fellowship (DGE-0221664) and Sigma Xi Grants-in-Aid of Research (G200510101920132434) for their support. This work is supported by the NRC/US AFOSR Summer Faculty Fellowship and NSF CAREER Award (DMR-0239415). Synchrotron experiments were conducted at beamline X27C, NSLS in Brookhaven National Laboratory supported by DOE. We thank Prof. B.S. Hsiao and Dr. Lixia Rong for facilitating the synchrotron X-ray measurement.

References

[1] Joannopoulos JD, Villeneuve PR, Fan S. Nature 1997;386:143–9.
[2] Xia YN, Gates B, Yin YD, Lu Y. Adv Mater 2000;12:693–713.
[3] Foulger SH, Kotha S, Seryda-Krawiec B, Baughman TW, Ballato JM, Jiang P, et al. Opt Lett 2000;25:1300–2.
[4] Fink Y, Urbas AM, Bawendi MG, Joannopoulos JD, Thomas EL. J Lightwave Technol 1999;17:1963–9.
[5] Adv Mater 2001;13:369–450 [special issue].
[6] Cumpston BH, Ananthavel SP, Barlow S, Dyer DL, Ehrlich JE, Erskine LL, et al. Nature 1999;398:51–4.
[7] Morkved TL, Lu M, Urbas AM, Ehrichs EE, Jaeger HM, Mansky P, et al. Science 1996;273:931–3.
[8] Angelescu DE, Waller JH, Adamson DH, Deshpande P, Chou SY, Register RA, et al. Adv Mater 2004;16:1736.
[9] Kim SO, Solak HH, Stoykovich MP, Ferrier NJ, de Pablo JJ, Nealey PF. Nature 2003;424:411–4.
[10] Stoykovich MP, Muller M, Kim SO, Solak HH, Edwards EW, de Pablo JJ, et al. Science 2005;308:1442–6.
[11] Bunning TJ, Natarajan LV, Tondiglia VP, Sutherland RL. Annu Rev Mater Sci 2000;30:83–115.
[12] Escuti MJ, Qi J, Crawford GP. Opt Lett 2003;28:522–4.
[13] Moon JH, Yang S, Yang SM. Appl Phys Lett 2006;88:121101–3.
[14] Choi T, Jang JH, Ullal CK, LeMieux MC, Tsukruk VV, Thomas EL. The elastic properties and plastic behavior of two-dimensional polymer structures fabricated by laser interference lithography. Adv Funct Mater 2006;16:1324–30.
[15] Colburn WS, Haines KA. Appl Opt 1971;10:1636–41.
[16] Gambogi WJ, Weber AM, Trout TJ. SPIE Proc 1994;2043:2–13.
[17] Smothers WK, Moroe BM, Weber AM, Keys DE. SPIE Proc 1990; 1212:20–9.
[18] Tondiglia VP, Natarajan LV, Sutherland RL, Tomlin D, Bunning TJ. Adv Mater 2002;14(3):187–91.
[19] Campbell M, Sharp DN, Harrison MT, Denning RG, Turberfield AJ. Nature 2000;404:53–6.
[20] Sutherland RL, Tondiglia VP, Natarajan LV, Chandra S, Tomlin D, Bunning TJ. Opt Express 2002;10:1074–82.
[21] Vaia RA, Dennis CL, Natarajan LV, Tondiglia VP, Tomlin DW, Bunning TJ. Adv Mater 2001;13(20):1570–4.
[22] Li CY, Birnkrant MJ, Natarajan LV, Tondiglia VP, Lloyd PF, Sutherland RL, et al. Soft Matter 2005;1:238–42.
[23] Zhu L, Cheng SZD, Calhoun BH, Ge Q, Quirk RP, Thomas EL, et al. J Am Chem Soc 2000;122:5957–67.